ANTENNA COMPLEX FOR LASER SENSING OF THE UPPER ATMOSPHERIC LAYERS

B.V. Kaul

Institute of Atmospheric Optics,
Siberian Branch of the Russian Academy of Sciences, Tomsk
Received December 17, 1991

Some parameters of the antenna complex of the station for high–altitude laser sensing of the atmosphere developed at the Institute of Atmospheric Optics of the Siberian Branch of the Russian Academy of Sciences are presented. The antenna complex is a part of a large multipurpose lidar which is currently under development. The main element of complex is a parabolic mirror 2205 mm *in diameter. In addition to the main goal of increasing the sensing range the design of the antenna complex is also aimed at providing:*

– versatility understood as a possibility of simultaneous application of laser sensing techniques based on recording the signal of elastic scattering at several wavelengths, including differential absorption methods and Raman scattering techniques;

– operation under conditions of high levels of background noise corresponding to light summer nights and to illumination of a city;

– operation under severe climatic conditions of winter.

This paper is devoted to the discussion of starting premises and measures adopted to achieve these goals.

1. INTRODUCTION

For lidar studies of the middle and upper atmospheric layers one has to have lidar facilities possessing sufficiently high energy potential. This term being quite understandable intuitively can be qualitatively described based on the approach devoloped in Refs. 1 and 2. According to Ref. 2, the function $F(\rho,)$ which is inversely proportional to the time required for obtaining a lidar return from an atmospheric layer $\Delta(r)$ with the preset SNR ξ, is defined by the formula

$$F(\rho) = \rho\Delta\xi^{-2} K_1 \left[1 + B_\lambda K_2/\rho + K_3/\rho\right]^{-1} , \quad (1)$$

where B_λ is the spectral brightness of the background, K_1, K_2, and K_3 are the generalized parameters of the lidar. The argument ρ of the function $F(\rho)$ is a generalized target parameter

$$\rho(r) = \beta_\pi(r)\, T^2(r)/r^2 , \quad (2)$$

where $\beta_\pi(r)$ is the backscattering coefficient and $T(r)$ is the atmospheric transparency along the path segment $[0, r]$.

The generalized lidar parameters are represented in terms of its technical characterics by the following formulas:

$$K_1 = 2E f S\eta/h\nu\,(1 + \kappa^{-1}) ; \quad (3)$$

$$K_2 = \Omega\Delta\lambda/cE ; \quad (4)$$

$$K_3 = h\nu n_d/c\eta ES(\kappa^2 + \kappa) , \quad (5)$$

where c is the speed of light, $h\nu$ is the photon energy, E is the energy of the laser pulse, f is the repetition frequency of laser pulses, S is the area of the receiving antenna, η is the total efficiency of the entire optical train, κ is the quantum efficiency of the photodetector, Ω is the solid angle of the directional pattern of the lidar receiver, $\Delta\lambda$ is the bandwidth of the lidar's optical train, n_d is the mean dark–count rate of the photodetector.

It seems to be natural to define the energy potential of the lidar by the quantity K_1, which determines the function $F(\rho)$ without the background ($B_\lambda = 0$) and dark current ($n_d = 0$) and for unity parameters of the target ρ, the spatial resolution Δr, and the signal–to–noise ratio ξ.

Thus, the energy potential of the lidar characterizes the data sampling rate limited only by quantum fluctuations of the optical signal. In other words this is a theoretical limit of the lidar detection capability. A degree of proximity to this limit is determined by the conditions

$$B_\lambda K_2/\rho \ll 1 ; \quad K_3/\rho \ll 1 . \quad (6)$$

The above–given formulas (1)–(6) vividly demonstrate the effect of certain technical parameter on the functional capabilities of the lidar and are convenient for use in lidar design. In particular, it can be easily seen from the superficial analysis of these formulas that the pulse energy E is the only parameter which affects all three generalized parameters of the lidar. Its increase improves the energy potential K_1 and simultaneously lowers the levels of external K_2 and internal K_3 noise.

One more way to improve the energy potential of the lidar is to enlarge the area of the receiving antenna. However, it should be noted at once that this way is not optimal as concerning the expenses. In addition it yields a growth of the weight and overall dimensions disproportionate to the resultant increase in the energy

0235-6880/92/04 277-05 $02.00

potential K_1. For these reasons the use of the large receiving antennas can be considered acceptable only if there are no other ways of increasing the potential K_1. It is also quite clear that lidars with the receiving mirror more than 1 m in diameter remain still unique and it is expedient to make them multipurpose in order to provide a possibility of solving simultaneously several problems. The versatility is also important from the viewpoint of an integrated approach to lidar studies of the atmosphere based on the use of different lidar techniques for investigation of interrelations of different atmospheric parameters and interactions of the atmospheric components.

2. OPTICAL ARRANGEMENT AND PARAMETERS OF THE ANTENNA COMPLEX

When designing the lidar complex as a whole we preset the only initial parameter, that is, the diameter of the primary mirror (D = 2.205 m), which was determined by the productive capacity. The rest of the parameters of the complex were chosen to make a compromise among the financial and productive capabilities and the need for the development of the multipurpose lidar capable of efficient operation under conditions of high levels of background noise and in severe climate.

Versatility of the lidar is achieved by the use of a multilobe directional pattern.[3] Optical arrangement is shown in Fig. 1.

The seven–lobe directional pattern of the antenna is formed by the six field–of–view diaphragms *10* arranged in the focal plane of the primary mirror *4* in a circle circumscribed about the principial focus. The seventh diaphragm (diaphragm of the axial channel) is formed by the entrance slit of the monochromator *6* illuminated by means of the system of mirrors *5*. The radiation of the laser transmitter of the axial channel *1* is directed, with the help of the system of mirrors *3*, into the atmosphere along the principal optical axis of the receiving antenna while the axes of the laser beams of the transmitters of the other six channels *7* are deflected at an angle of 0.5° with respect to the principal optical axis of the primary mirror in its meridional plane by the mirrors *9*. As a result of such an optical arrangement of the directional patterns of the transmitters the images of corresponding scattering volumes at infinity lie in a circle in which the field–of–view diaphragms are arranged. Photodetectors are placed just behind the focal plane in order to avoid certain losses of radiation and to improve the stability of the system against missalignments by eliminating "excessive" optical parts. To service the photodetector block in the course of alignment and repairing a special removable platform is used. This platform being moved out shades about 20 % of the antenna receiving area. In normal operational regime the platform is removed. The block of photodetectors shades about 4 % of the area of the mirror. To align the directional pattern of the transmitter in the direction corresponding to the position of the field–of–view diaphragm corresponding to this transmitter we use the special optical unit *14* for the beam transfer. This unit is made in the form of an optical bench rotating about the optical axis of the primary mirror. When adjusting the lidar the bench is placed in the meridional plane of the primary mirror that passes through the centers of the field–of–view diaphragm and of the aperture of the laser. The part of the laser beam is intercepted by the unit *14*. Upon entering this unit two beams are formed parallel to the input beam. By adjusting the position of the mirror *9* the output beams are directed in such a way that after reflection from the primary mirror they intersect at the center of the diaphragm *10*.

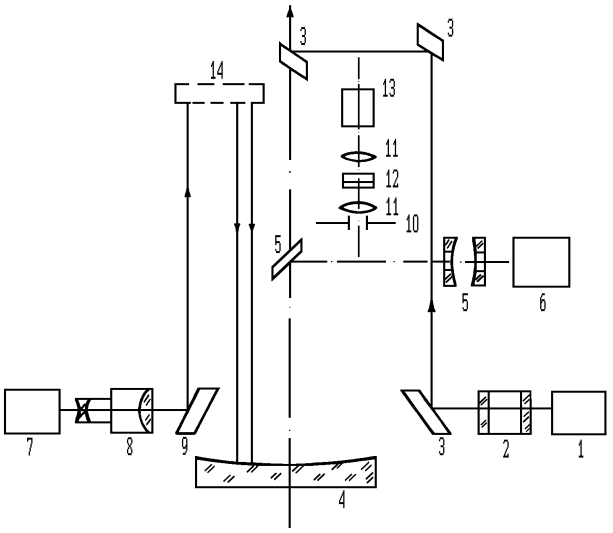

FIG. 1. Optical arrangement of the antenna complex: 1) laser transmitter of the axial channel, 2) hermetic input of radiation in the silo of the antenna complex, 3) deflecting mirrors, 4) primary mirror, 5) deflecting and adjusting mirrors for illumination of the entrance slit of a monochromator, 6) monochromator, 7) laser transmitter of one of the six possible off–axis channels, 8) collimator which is also employed as a hermetic optical input of radiation in the silo, 9) deflecting mirror, 10) field–of–view diaphragm, 11) lenses, 12) interference filter, 13) photodetector, 14) unit used to transfer the radiation for alignment of the off–axis channels.

Starting from the principle accepted for the optical arrangement of the lidar let us formulate certain requirements for the parameters of the primary mirror.

From Eq. (4) it follows that the most stringent requirements must be emposed on the quality of manufacturing the surface of the optical parts. Only this way can provide the possibility for obtaining very narrow directional patterns thereby improving the spatial selection of the background. Of course, several circumstances impose limitations on realization of this possibility and, as a consequence, certain compromise should be found.

First of all, it should be kept in mind that the discussed optical arrangement uses the off–axis beams; therefore, the optical image of the scattering volume will be distorted due to the aberrations. Second, very narrow directional patterns of the six off–axis chanels may result in unacceptably extended shadow and transition zones, though this difficulty can be overcome. A more significant disadvantage is that the requirements for the high quality of the mirror and realization of extremely narrow directional patterns substantially rise the expense of the primary mirror itself and of the mechanical construction supporting it because of the temperature and other drifts, which must be carefully controlled in this case.

When choosing an acceptable radius of curvature of the mirror surface we aimed at obtaining such a diameter of the aberration circle which would provide the possibility of arranging the photodetectors of the off–axis channels in direct focus for the diversity directional patterns. As the analysis of aberrations of a parabolic mirror shows the main contribution to the distortions due to aberrations comes from coma, provided that the observation point is but slightly displaced from the principal focus. The maximum diameter of coma aberration circle d_c is given by the formula

$d_c = 3D^2L/16f^2$,

where D is the diameter of the primary mirror, f is its focal length, and L is the displacement of the image of a point source from the principal focus in the focal plane.

Since the diameter of the primary mirror is preset and the decrease of L is limited by the size of the photodetectors and accompanying constructions we may vary only the focal length f, whose increase minimizes the coma aberration. On the other hand, the value of f is also limited by the height of the silo in which the antenna complex is arranged.

Thus, taking into account the above–mentioned considerations the focal length was taken to be 10 m (the manufacturer made a focal length of 10.07 m). As a result, the radius of a circle (L) in which the field–of–view diaphragms were arranged was 87.5 mm, and the corresponding diameter of the circle of coma aberration was 0.75 mm, which was regarded quite admissible. In this case the quality of the mirror surface should provide the diameter of the least circle of blurring of the image of the point source being equal to 750 mm, which substantially decreased the time and expense of polishing the mirror. Actual diameter of the least circle of blurring was 500 mm. As a consequence, the limiting angular apertures due to aberrations were equal to $5\cdot10^{-5}$ rad for the axial channel and to $7.5\cdot10^{-5}$ rad for the off–axis channels.

In fact, the angular apertures currently used are about $3\cdot10^{-4}$ rad, that is, by an order of magnitude larger than the limitiag values. In this case no special measures are needed for stabilization of the spatial positions of the receiving and transmitting angular apertures under conditions of diurnal temperature variations. Of course, the possibility of improving the spatial selection of the background by narrowing the angular apertures still remains.

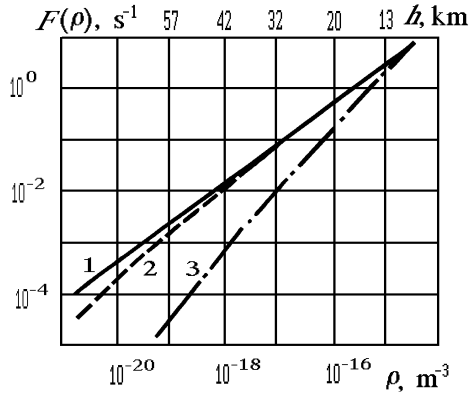

FIG. 2. Family of the characteristics of the lidar $F(\rho, B)$ *for the laser with* $E = 1$ J *per pulse at a pulse repetition rate of* 1 Hz. *The technical characteristics of the antenna complex are:* $S = 3.6$ m^2, $\eta = 0.3, \Omega = 2.12\cdot10^{-7}$ sr, ($\varphi = 3\cdot10^{-4}$ rad), $\Delta\lambda = 10^{-3}$ μm, *the quantum efficiency of the photodetector* $\kappa = 0.05$, *and the dark–count rate of the photodetector is* 10^2 s^{-1}. *The generalized parameters of the lidar are* $K_1 = 2.75\cdot10^{17}$ m$^2\cdot$s^{-1}, $K_2 = 7.07\cdot10^{-19}$ W^{-1}sr$\cdot$μm$\cdot$m^{-1}, *and* $K_3 = 2.31\cdot10^{-24}$ m^{-3}. $B_\lambda = 10^{-6}$ (*curve* 1), 10^{-3} (*2*), *and* 1 W$\cdot$sr$^{-1}\cdot$μm$^{-1}\cdot$m^{-2}(*3*).

As has already been noted above, the applicability of the lidar for solving a certain problem can be characterized by the function $F(\rho)$ given by formula (1). This function calculated for the laser pulse energy of 1 J with a pulse repetition rate of 1 Hz is shown in Fig. 2 to illustrate the capabilities of the lidar which is currently under construction. Other parameters of the lidar are chosen so as they have already been realized or are expected to be realized in one or other channel. Their values are given in the figure caption. In calculations of the function shown in Fig. 2 we set the SNR ξ is equal to 100 and the spatial resolution Δr to 100 m. To obtain $F(\rho)$ for other values of these parameters its values must be multiplied by the factor $k = 10^2\xi^{-2}\Delta r$.

At the top of Fig. 2 shown graphically is the altitude scale corresponding to the values of the generalized target parameter ρ for which we have assumed a standard molecular atmosphere. As can be seen from this figure a lidar return due to Rayleigh scattering can be recorded at an altitude of 70 km with the 100 m spatial resolution and the SNR equal to 100, during the integration time of about $2\cdot10^3$ s. An increase of the range of spatial averaging from 100 m to 1 km yields a reduction of the integration time to 200 s, that is quite acceptable. In order to extend the sensing range up to 100 km with the same value of the SNR, the average power of the laser must be increased by about an order of magnitude. On the other hand, if the SNR of 10 and spatial resolution of 1 km are admissible, these altitudes could be attained with the laser energy taken in the above–presented calculations, namely, with the laser emitting 1 J per pulse with the pulse repetition rate of 1 Hz. It can be seen from the figure that the effect of the background at the level $B_\lambda \simeq 10^{-3}$ W/μm$\cdot$m$^2\cdot$sr, corresponding to a moon night, is insignificant (curve *2*). At the same time, the effect of the background at the level $B_\lambda = 1$ W/μm$\cdot$m$^2\cdot$sr before sunrise or after sunset, would require to prolong the integration time by an order of magnitude for a sensing range of 40 km (see curve *3*), which by the way is still acceptable.

Of course, it should be kept in mind that to operate during light time, we need a photodetector capable of working at high background level.

3. GEOMETRIC FUNCTION OF THE ANTENNA COMPLEX

As a result of large aperture and long focal length of the antenna complex, the extended shadow and transition zones are formed in which the signal first rises and then falls down disproportionate to the squared range. The shadow zone of the axial channel is formed due to the screening of a singly scattered radiation by the block of detectors. If the receiving and transmitting angular apertures are $3\cdot10^{-4}$ rad and $1.5\cdot10^{-4}$ rad and the initial diameter of the laser beam is 0.15 m, then the length of this zone is about 550 m. The transition zone next to the zone of shadowing is caused by vignetting of the rays incident on the primary mirror at the angles $\Psi > d/2f$ by the field–of–view diaphragm of the diameter d, as well as by vignetting due to displacement of the image of the scattering volume from the postfocal space toward the focus. For the 10 m focal length such a displacement amounts to about 1 mm for the scattering volume at a distance of 100 km. The displacement of the image amounts to about 100 mm for the scattering volume at a distance of 1 km. The vignetting can be neglected if the condition

$$f(\varphi + D/r) < d$$

is satisfied. Here φ is the angular divergence of the sounding beam, D is the diameter of the primary mirror, r is the sensing range, and d is the diameter of the field–of–view diaphragm. If the diaphragm is 3 mm in diameter and $\varphi = 1.5\cdot10^{-4}$ rad this condition will be satisfied starting from the altitude of 15 km. The length of the transition zone can be shortened by displacing the field–of–view diaphragm bchind the focal plane. This effect is illustrated by Fig. 3 where the geometric functions of the axial channel calculated for the field–of–view diaphragm placed in the focal plane and displaced at a

distance of 10 μm behind it are shown. Note that the geometric function $G(r)$ is defined as the ratio

$$G(r) = \omega'(r)/\omega(r) ,$$

where $\omega'(r)$ is the effective solid angle and $\omega(r) = \pi D^2/4\, r^2$.

The calculations were made assuming a uniform distribution of the beam energy over the beam cross section. For this reason the actual shape of the geometric function will differ slightly from that shown in the figure.

For the off–axis channels the shadow and transition zones are formed due to radial and axial displacements of the image of the scattering volume as it moves along the sounding path. For the same receiving and transmitting angular apertures ($\Psi = 3\cdot 10^{-4}$ rad and $\varphi = 1.5\cdot 10^{-4}$ rad) the shadow zone terminates at a distance of 5.3 km and the transition zone terminates at a distance of 16 km.

Such an extended shadow and transition zones have both advantages and disadvantages. The main disadvantage is that it is difficult to control the geometric function. Even when we succed in calculating or measuring the geometric function, small misalignments of the laser resonator engendering the change in the distribution of the energy over the beam cross section or small deviations of the receiving and transmitting angular apertures relative to each other can have a significant effect on the form of the function $G(r)$.

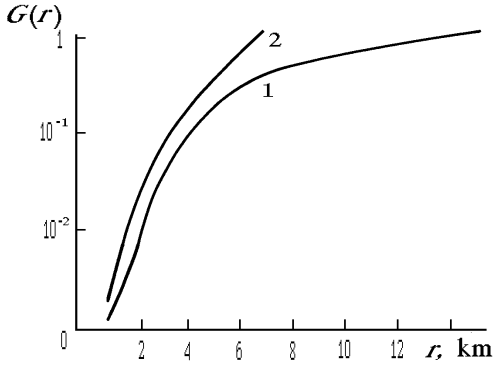

FIG. 3. Geometric function of the axial channel: 1) diaphragm is placed in the focal plane and 2) diaphragm is displaced along the axis at a distance of 10 μm *in the postfocal space.*

For these reason the interpretation of data on laser sensing is difficult for the altitude range corresponding to the transition zone if it requires the direct solution of the lidar equation. At the same time this difficulty is avoided in differential absorption and Raman scattering techniques since in these methods the ratios of simultaneously recorded lidar returns are used to retrieve the atmospheric parameters. In this case the extended transition zone of the lidar with long focal length of the receiver becomes very advantageous because it reduces the dynamic range of return signals and eliminates the intense illumination of photodetectors. A possibility of regulating the shape of the geometric function by axial displacement of the field–of–view diaphragm is also an advantage of this system. Since the axial channel of this lidar was initially designed as a Raman–lidar channel, its transition zone is almost optimal.

The off–axis channels of the lidar are used for sounding ozone at altitudes of from 20 to 50 km, for multifrequency laser sensing of aerosol, and for retrieving the air temperature and density at altitudes of from 80 to 100 km. To avoid the effect of intense illumination from the subjacent layers (below 15–20 km), the use of an electromecanical cutoff is assumed. In this case the shapes and extensions of the shadow and transition zones have no fundamental significance.

4. SPECIFIC FEATURES OF THE LIDAR DESIGN

A building of the lidar station and especially the design of its antenna complex take into account severe climatic conditions of winters. All optical parts of the transmitting antennas, photodetector block, and alignment units are assembled on a common metal truss supported by a concrete monoblock which is also used as a basis for the carriage of the primary mirror. This monoblock is supported by a pad of a sand and gravel mixture being thus completely insulated from the main building. The whole construction of the antenna complex is enclosed in a 6×6 m silo, which is thermally insulated from surrounding heated rooms of the building. The silo is connected with the surrounding rooms by hermetic tambours. Housing of the silo inside the heated building and thermal insulation of the upper part of the concrete monoblock are used to avoid the displacements of antenna complex due to freezing of soil.

The silo is equipped with the forced supercharging system used to homogenize the temperatures inside the silo with the outdoor air temperature. The primary mirror is fabricated from the SO 115M glass ceramic which has a very low thermal expansion coefficient. The mirror is supported by 18 bearings of the Lassel system. The design of these bearings is used not only to unload the mirror but also to compensate for the difference between the thermal expansion of the mirror and its mount. Laser sources, recording electronics, and other auxiliary instrumentation of the lidar are in the surrounding rooms. Laser radiation enters the silo either through the hermetic optical windows *2* (see the optical arrangement) or through the collimator inserted in a hermetic hatches in the walls of the silo. The collimators are equipped with the systems of air heating and drying in order to protect the surfaces of optical parts againts water vapor condensation.

5. CONCLUSION

The experimental use of this antenna complex has shown that the adopted measures are quite sufficient for its efficient operation. At present the channels for sounding the atmospheric density and aerosol stratification at $\lambda = 532$ and 694 nm have already been tested. Also we have performed the channel for sensing of the atmospheric temperature profiles on the basis of the rotational Raman scattering spectra. The works on increasing the functional capabilities of the lidar and modification of its systems are still ccarrying on.

The author would like to note that the development of the above–described complex being a part of the Station of laser sensing of the atmosphere was initiated by Academician V.E. Zuev and performed under his leadership and with his assistance. The project of the antenna complex was designed in Special Design Office of Scientific Instrumentation "Optika" of the Siberian Branch of the Russian Academy of Sciences. The majority of the engineering solutions belongs N.A.Agapov, S.A.Danichkin, I.G.Polovtsev, E.B.Tskhai, et al.

The work on the development of multipurpose lidar on the basis of this antenna complex and experimental use of this lidar was done by the staff of the Laboratory of high–altitude sensing of the atmosphere.

REFERENCES

1. V.E. Zuev, B.V. Kaul, I.V. Samokhvalov, et al., *Laser Sensing of Industrial Aerosols* (Novosibirsk, Nauka, 1986).
2. B.V. Kaul, Atm. Opt. **2,** No. 2, 166–169 (1989).
3. B.V. Kaul, "*Multiwavelength lidar for sensing of the atmosphere*", Inventar's Certificate No. 1345861 (SSSR) MKI G01W1/00.